



SCUOLA INTERNAZIONALE SUPERIORE DI STUDI AVANZATI

SISSA Digital Library

Non-Fermi-liquid behavior in quantum impurity models with superconducting channels

Original

Non-Fermi-liquid behavior in quantum impurity models with superconducting channels / Zitko, Rok; Fabrizio, Michele. - In: PHYSICAL REVIEW. B. - ISSN 2469-9950. - 95:8(2017), pp. 1-10. [10.1103/PhysRevB.95.085121]

Availability:

This version is available at: 20.500.11767/48569 since: 2023-08-08T10:03:55Z

Publisher:

Published

DOI:10.1103/PhysRevB.95.085121

Terms of use:

Testo definito dall'ateneo relativo alle clausole di concessione d'uso

Publisher copyright

APS - American Physical Society

This version is available for education and non-commercial purposes.

note finali coverpage

(Article begins on next page)

Non-Fermi-liquid behavior in quantum impurity models with superconducting channels

Rok Žitko^{1,2} and Michele Fabrizio³

¹*Jožef Stefan Institute, Jamova 39, SI-1000 Ljubljana, Slovenia*

²*Faculty of Mathematics and Physics, University of Ljubljana, Jadranska 19, SI-1000 Ljubljana, Slovenia*

³*International School for Advanced Studies (SISSA), and CNR-IOM Democritos, Via Bonomea 265, I-34136 Trieste, Italy*

(Dated: October 10, 2018)

We study how the non-Fermi-liquid nature of the overscreened multi-channel Kondo impurity model affects the response to a BCS pairing term that, in the absence of the impurity, opens a gap Δ . We find that non-Fermi liquid features do persist even at finite Δ : the local density of states lacks coherence peaks, the states in the continuum above the gap are unconventional, and the boundary entropy is a non-monotonic function of temperature. Even more surprisingly, we also find that the low-energy spectrum in the limit $\Delta \rightarrow 0$ actually does not correspond to the spectrum strictly at $\Delta = 0$. In particular, the $\Delta \rightarrow 0$ ground state is an orbitally degenerate spin-singlet, while it is an orbital singlet with a residual spin degeneracy at $\Delta = 0$. In addition, there are fractionalized spin-1/2 sub-gap excitations whose energy in units of Δ tends towards a finite and universal value when $\Delta \rightarrow 0$; as if the universality of the anomalous power-law exponents that characterise the overscreened Kondo effect turned into universal energy ratios when the scale invariance is broken by $\Delta \neq 0$. This intriguing phenomenon can be explained by the renormalisation flow towards the overscreened fixed point and the gap cutting off the orthogonality catastrophe singularities.

PACS numbers: 72.15.Qm, 75.20.Hr

The density of states (DOS) $\rho(\omega)$ of a conventional BCS s -wave superconductor has a gap Δ and coherence peaks above, $\rho(\omega) = \rho_0 \text{Re} \omega / \sqrt{\omega^2 - \Delta^2}$, where ρ_0 is the normal-state DOS. This remains true also in the presence of disorder and impurities that maintain time-reversal invariance¹. By contrast, magnetic impurities may induce additional states inside the gap by binding Bogoliubov quasiparticles through the exchange coupling J^{2-4} . The bound-state energies depend on the interplay of Kondo screening, superconducting proximity effect, and spin-orbit coupling⁵⁻⁷, and are measurable in hybrid superconductor-semiconductor nanostructures⁸⁻¹⁰ and adsorbed magnetic atoms or molecules¹¹⁻¹³. In the limit of small gap, $\Delta \rightarrow 0$, the sub-gap states induced by impurities that are Kondo screened (effectively non-magnetic) or under-screened (with a residual local moment decoupled from the rest of the system) move towards the gap edges and merge with the coherence peaks, because the weak superconducting pairing perturbs a system that was formerly in a (regular or singular) local Fermi liquid (FL) state¹⁴⁻¹⁶. The effect of the impurity on the bulk electrons is thus fully accounted by the quasiparticle scattering phase shifts resulting from the Kondo effect ($\pi/2$ in the deep Kondo limit)¹⁷. There is, however, a further class of quantum impurities that are Kondo over-screened because the number of screening channels k exceeds twice the impurity spin $2S$ ¹⁸⁻²⁰. Such overcompensation has been experimentally demonstrated for the two-channel Kondo model ($k = 2, S = 1/2$) in artificial semiconductor quantum dot devices²¹⁻²⁴. The resulting states are non-Fermi liquids (NFL)^{19,25} with excitation spectra that deviate significantly from the FL paradigm, but can be still described in terms of appropriate boundary conformal field theories²⁶⁻²⁹. When a small gap is opened in the contacts of such systems, the superconducting state thus emerges out of a non-Fermi liquid. Two related questions arise: 1) What is the nature of the excitations forming the continuum above the gap? 2) Can the sub-gap states be interpreted as bound states of NFL excita-

tions?

In this work the problem is studied using the numerical renormalization group (NRG) technique³⁰⁻³³ and analytical arguments. For the two-channel Kondo (2CK) model³⁴ in the limit $\Delta \rightarrow 0$ we find surprisingly that the low energy spectrum does not reproduce that at $\Delta = 0$: the ground state (GS) is a doubly degenerate spin-singlet, while two $S = 1/2$ sub-gap Shiba states become degenerate with a *universal dimensionless energy ratio*

$$\epsilon^* \equiv E^* / \Delta \approx 0.5983. \quad (1)$$

In other words, even in the $\Delta \rightarrow 0$ limit these bound states do not merge with the continuum. The excitations above the gap have NFL degeneracies and spacing, and there are no coherence peaks in the impurity DOS. When the NFL regime is disrupted by breaking the channel degeneracy^{19,35}, the sub-gap states do move toward the gap edge and the coherence peaks are restored when the FL-NFL cross-over scale T^* exceeds Δ .

We consider the Hamiltonian $H = \sum_{i=1}^k J_i \mathbf{s}_i \cdot \mathbf{S} + H_i$, where

$$H_i = \sum_{k\sigma} \epsilon_k c_{i,k\sigma}^\dagger c_{i,k\sigma} + \sum_k \left(\Delta c_{i,k\uparrow}^\dagger c_{i,k\downarrow}^\dagger + \text{H.c.} \right), \quad (2)$$

i.e., a k -channel Kondo model¹⁹ with each channel described by a BCS mean-field Hamiltonian with fixed Δ . J_i is the exchange coupling, \mathbf{s}_i is the spin density of channel- i electrons at the position of the impurity, \mathbf{S} is the impurity spin- S operator, and finally $c_{i,k\sigma}^\dagger$ creates an electron in channel- i with momentum k , spin σ , and energy ϵ_k . The continuum has a flat DOS with half-bandwidth D , i.e., $\rho_0 = 1/2D$. The Kondo scale for small exchange coupling is $T_K \approx \exp(-1/\rho_0 J_{\text{avg}})$, where $J_{\text{avg}} = \sum_i J_i / k$ ³⁶. If J_i are non-equal, there is further relevant scale T^* that grows as a power law with the difference between the two largest J_i ³⁴. For $\Delta = 0$, the system has

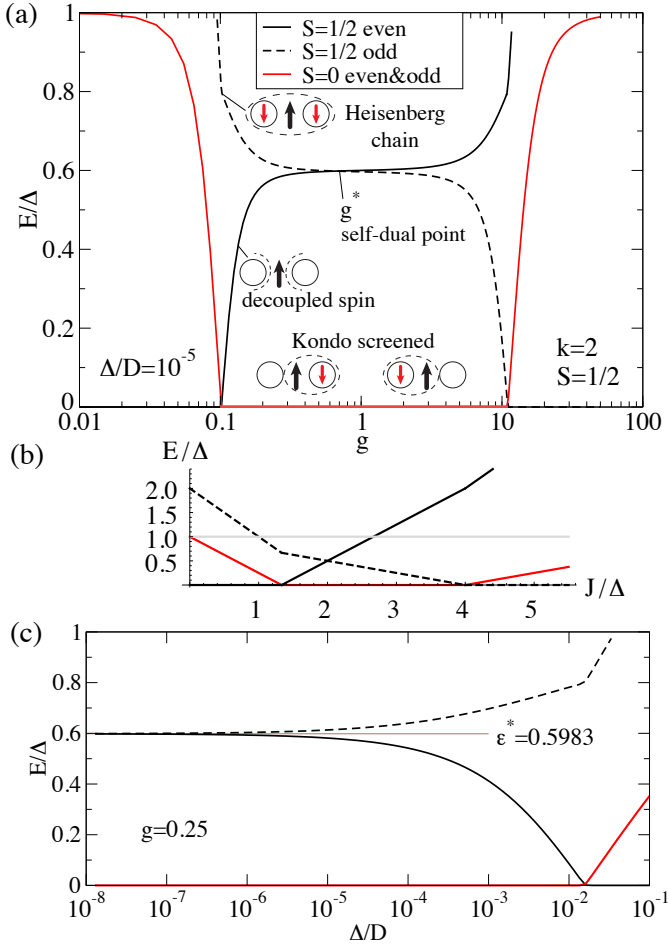


Figure 1. (a) Sub-gap many-particle states in the 2CK model with fixed gap as a function of $g = \rho_0 J$. The energies are given with respect to the ground-state energy. (b) Eigenstates in the zero-bandwidth limit. (c) Approach toward the asymptotic universal spectrum in the zero-gap limit.

NFL properties for $T^* < T < T_K$ and crosses over to a FL GS for $T < T^*$. For $\Delta \neq 0$, we use the NRG to compute the finite-size excitation spectra, thermodynamic properties, and the T -matrix spectral function (impurity DOS).

The discrete (sub-gap) part of the excitation spectrum for the 2CK model with $J_1 = J_2 = J$ is shown in Fig. 1(a) at constant gap Δ as a function of the dimensionless coupling constant $g = \rho_0 J$. To better understand the origin of these states, we introduce a simplified zero-bandwidth model where each screening channel is represented by a single orbital f_i with pairing ($\Delta f_{i\uparrow}^\dagger f_{i\downarrow}^\dagger + \text{H.c.}$), and $2s_i = \sum_{\alpha\beta} f_{i\alpha}^\dagger \sigma_{\alpha\beta} f_{i\beta}$. The lowest four eigenstates, shown in Fig. 1(b), are in qualitative correspondence with those of the full model. The even-parity $S = 1/2$ state represents a decoupled impurity spin. (The parity refers to the channel inversion symmetry.) This is the GS for low g and corresponds to the local-moment phase at $\Delta > T_K$. Each spin-singlet state corresponds to the impurity spin coupled into an $S = 0$ state to a singly-occupied orbital, the other orbital being instead in the configuration $(|0\rangle - |\uparrow\downarrow\rangle)/\sqrt{2}$. There are evidently two such spin-singlet

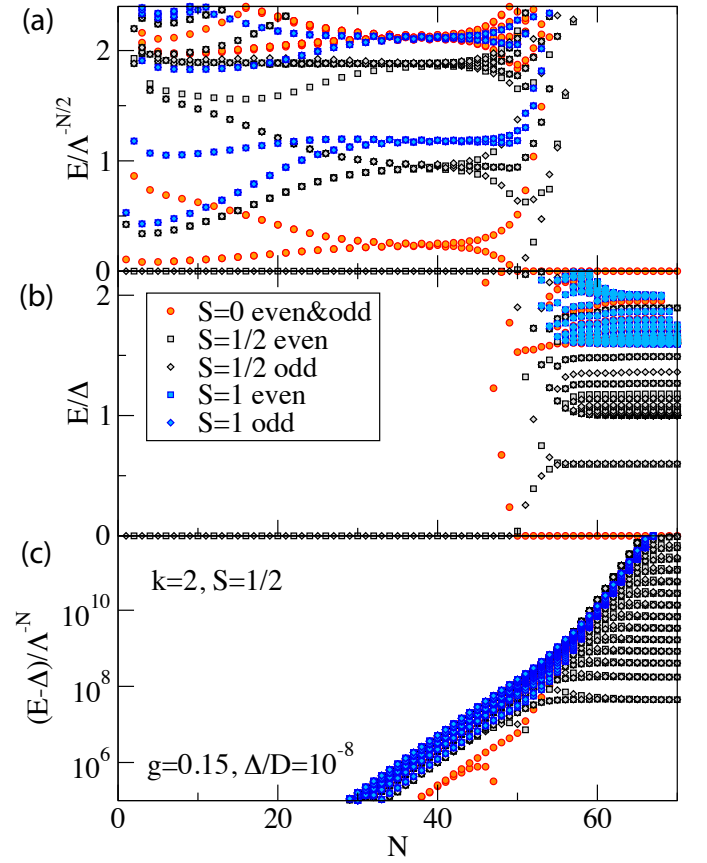


Figure 2. Renormalization flow diagram with different scalings of the energy axis. N is the iteration number and $\Lambda = 2$ is the NRG discretization parameter.

states, depending on which orbital screens the impurity. This is actually the doubly degenerate GS for intermediate values of g . Finally, in the large- g limit the GS is an odd-parity strong-coupling state: both orbitals are singly occupied and coupled into an odd-parity spin-triplet configuration, which is in turn coupled to the impurity into a $S = 1/2$ state. The low- g and high- g limits are related through a duality mapping which interchanges the parity of the $S = 1/2$ states and which also occurs in the $\Delta = 0$ model^{35,36}. At $g = g^* \approx 0.7$ these states cross and thereby define the self-dual point. This occurs at a particular value of the excitation energy ϵ^* defined in Eq. (1). This value is actually universal: for any g the two doublet levels converge in the $\Delta \rightarrow 0$ limit toward the same value ϵ^* , see Fig. 1(c). The self-dual point thus defines the universal non-trivial fixed point of the theory in the small-gap limit, as well as at $\Delta = 0$. The approach toward this limit is a square-root function of Δ :

$$E_{o,e}/\Delta \sim \epsilon^* + c_{o,e}(g)\Delta^{1/2}. \quad (3)$$

Magnetic anisotropy $J_\perp \neq J_z$ is irrelevant, as in the normal state, and does not affect the value of ϵ^* .

In Fig. 2 we show the finite-size excitation spectrum (NRG flow diagram) as a function of the Wilson chain length N , corresponding to the energy scale $\epsilon_N = \Lambda^{-N/2}$. Specif-

ically, Fig. 2(a) reports the energies scaled as $\epsilon = E/\epsilon_N$, and demonstrates the cross-over from the local-moment to the 2CK NFL fixed point for $N \gtrsim 30$, with characteristic fractional energies $\epsilon_N = 0, 1/8, 1/2, 5/8, 1, \dots$ and degeneracies $2, 4, 10, 12, 26, \dots$, respectively, that reflect the peculiar $SU(2)_2 \times SO(5)$ conformal field theory (CFT) that describes the asymptotic behaviour of the model at $\Delta = 0$ ^{26,29,34,37}. We observe that a finite Δ lowers the $SO(5)$ symmetry down to $SU(2) \times U(1)$, which corresponds to an $SU(2)_2$ CFT times the Z_2 orbifold of a compactified $c = 1$ CFT. The latter allows for a marginal boundary operator able to split the $SO(5)$ multiplets; for instance the degeneracy 4 of the $1/8$ state into $4 \rightarrow 2 + 2$, or the degeneracy 10 of the $1/2$ state into $10 \rightarrow 2 + 6 + 2$ ³⁷. Such splitting is already evident in Fig. 2(a) for $40 \lesssim N \lesssim 45$. However, for $N \gtrsim 45$, the BCS gap exceeds ϵ_N and induces flow toward a new fixed point which is better characterized by scaling the energies as E/Δ , see Fig. 2(b). The lowest doublet of the split $\epsilon = 1/8$ multiplet becomes the doubly degenerate spin-singlet GS, while the $\epsilon = 0$ $S = 1/2$ -state and the lowest $S = 1/2$ state of the split $\epsilon = 1/2$ multiplet meet into the $S = 1/2$ sub-gap doublet. The continuum of excitations for $E > \Delta$, which is dense close to the gap edge, is best shown scaled as $(E - \Delta)/\Lambda^{-N}$, Fig. 2(c). The energies are spaced by the ratio of Λ , rather than Λ^2 as in the gapped single-channel FL case^{37,38}. Such progression results from a combination of FL states with one channel having $\delta = 0$ and the other $\delta = \pi/2$ quasiparticle phase shift, as expected for a GS where the Kondo effect is formed with one channel, the other being decoupled. This does not imply, however, that FL behavior is recovered. The degeneracy of states above the gap is twice the number for a FL. More remarkably, when the matrix elements are evaluated to compute the impurity DOS, there are no coherence peaks (see below). The non-trivial effects are thus revealed chiefly through the matrix elements, rather than the energy-level spacing.

The reshuffling of states when the gap opens leads to peculiar thermodynamics. In Fig. 3 we plot the impurity magnetic susceptibility, χ_{imp} , and impurity (boundary) entropy s_{imp} . For $T \gg \Delta$, the temperature dependence equals that of the $\Delta = 0$ model: the effective local moment goes to zero and the impurity entropy reaches the $\ln 2/2$ plateau. At $T \sim \Delta$, the effective degeneracy of the impurity-generated states increases, leading to peaks in both χ_{imp} and s_{imp} . The boundary entropy thus increases from $\sim \ln 2/2$ to $\ln 2$. The g -theorem³⁹ does not hold here because Δ breaks the conformal invariance.

The FL properties are restored when the channel symmetry is broken. The sub-gap spectrum, shown in Fig. 4(a) as a function of $\Delta J = (J_1 - J_2)/2$ for constant J_{avg} such that $T_K \gg \Delta$, now depends on the relative value of Δ and the NFL-FL crossover scale T^* . For small ΔJ such that $T^* \ll \Delta$, the sub-gap spectrum is ‘‘NFL-like’’ with the $S = 1/2$ doublet close to ϵ^* . As ΔJ increases, the degeneracy between the spin-singlet states is lifted. The Kondo state in the dominant channel remains the GS, while the other Kondo state rapidly rises in energy and enters the continuum. The sub-gap $S = 1/2$ doublet asymptotically approaches the gap edge in the large ΔJ limit where $T^* \gg \Delta$, and the spectrum becomes ‘‘FL-like’’ with no

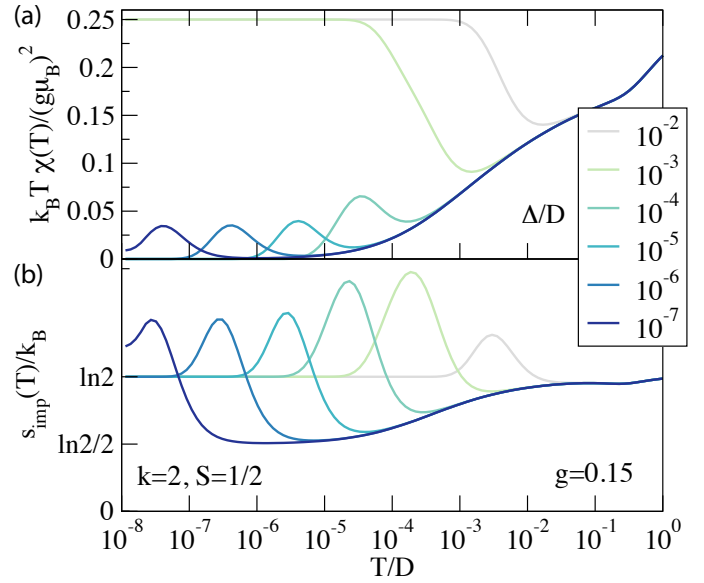


Figure 3. Temperature dependence of (a) impurity magnetic susceptibility and (b) impurity entropy.

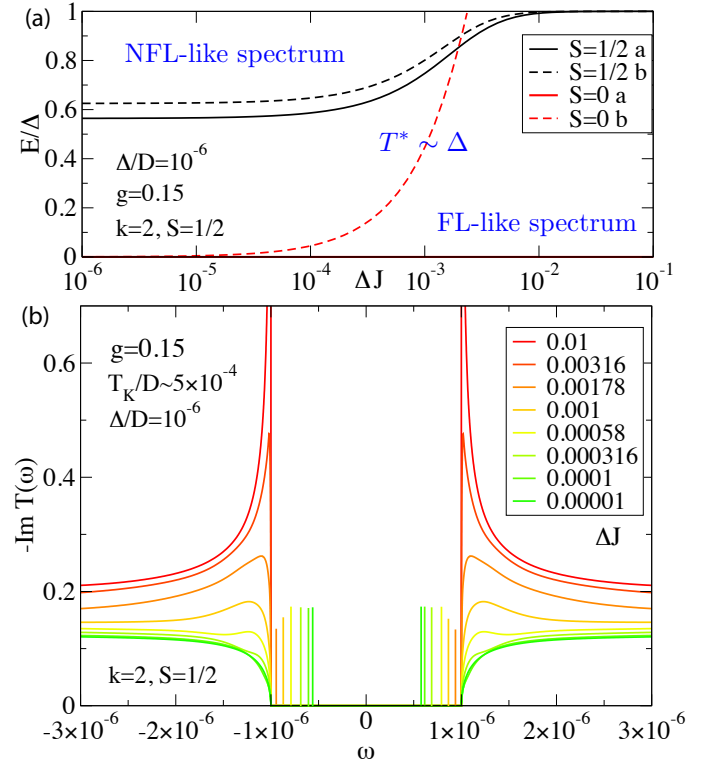


Figure 4. Channel symmetry breaking, $J_1 \neq J_2$. (a) Evolution of the sub-gap states vs. ΔJ ; the cross-over point $T^* \sim \Delta$ occurs for $\Delta J \approx 10^{-3}$. (b) Impurity spectral function (Im part of T -matrix) for a range of ΔJ .

sub-gap states (because $\Delta \ll T_K$). The NFL-FL crossover has a characteristic signature also in the impurity DOS, see Fig. 4(b): with increasing ΔJ , the δ -peaks move toward the continuum edges and the spectral weight is transferred from the sub-gap region into the continuum to form the coherence peaks characteristic of the FL regime.

We now sketch an analytical argument that explains qualitatively and to some extent also quantitatively the NRG results; details are provided as Supplemental Materials³⁷. At particle-hole symmetry, the Hamiltonian can be mapped onto a non-superconducting model in which the pairing potential is transformed into a staggered one with the same strength Δ , the advantage being that symmetries and quantum numbers are more transparent. In the same spirit as Anderson and Yuval⁴⁰⁻⁴², we start by the scattering problem at zero spin-flip exchange, $J_{\perp} = 0$. In this case, if the impurity spin is up, the spin up and down electrons feel a scattering potential $V_{\uparrow} = V$ and $V_{\downarrow} = -V$, respectively, where $V = J_z/4$. $V_{\uparrow(\downarrow)}$ changes sign if the impurity spin is reversed. In the spectrum of the electrons with spin opposite to the impurity, a channel-degenerate bound state appears whose energy

$$E_{\text{bound}} = \Delta \frac{1 - (\pi\rho V)^2}{1 + (\pi\rho V)^2}, \quad (4)$$

is located right in the middle of the gap at the self-dual point $(\pi\rho V)^2 = 1$. The ground state at $J_{\perp} = 0$ is therefore degenerate. If the impurity spin is up, there is a spin-down bound state right at the Fermi level that can be either empty or occupied at no energy cost, hence a degeneracy two for each channel. Analogously if all spins are reversed; hence an overall eightfold degeneracy. A finite J_{\perp} splits this degenerate subspace since it has a finite matrix element $\propto (\rho\Delta)^{3/2}$ between states with a single electron occupying the bound state with the same channel index but opposite spin. Inclusion of J_{\perp} at all orders corresponds in the Anderson and Yuval's approach to an infinite sequence of X-ray edge problems. However, in this circumstance the edge singularities are cut off by

the gap Δ , so that the effective low-energy model obtained by integrating out the high-energy states still comprises the above fourfold degenerate multiplet separated by a finite energy gap from higher energy states. Such low-energy multiplet is split as discussed above by an upward renormalised $J_{\perp}^* \simeq J_{\perp} (\Delta\rho)^{-1/2}$ into a lowest energy channel-degenerate spin-singlet, with singly occupied bound state, followed by two spin-1/2 states where the bound state is either empty or doubly occupied and next by a channel-degenerate spin-triplet still with singly occupied bound state, which however falls in the continuum above the gap. The energy difference between the two inside-gap states, the lowest spin-singlet and upper spin-1/2, is estimated as $(2/\pi)\Delta \approx 0.637\Delta$, surprisingly close to the actual value $\epsilon^* \approx 0.598$.

The three-channel Kondo (3CK) models show similar anomalies with multiple spin-doublet sub-gap states with universal energy ratios 0.19 and 0.72³⁷. The local DOS above the gap is anomalous, lacking the Fermi-liquid coherence peaks. We speculate that impurity models with Kondo overscreening generically flow in the small-gap limit to fixed points with characteristic persistent bound states of NFL character.

More generally, let us imagine to add the mass term Δ first at the impurity site. This term does not correspond to any of the relevant boundary operators at the NFL fixed point, nevertheless it lowers the symmetry and allows for a marginal boundary operator. If this is the case, we argue that an arbitrarily weak mass term of that kind added at the impurity site as well as in the bulk will induce sub-gap states with universal ratios. The predicted universal spectra are in principle empirically testable in quantum impurity systems.

ACKNOWLEDGMENTS

RŽ acknowledges the support of the Slovenian Research Agency (ARRS) under P1-0044 and J1-7259.

-
- ¹ P. W. Anderson, "Theory of dirty superconductors," *J. Phys. Chem. Solids* **11**, 26 (1959).
 - ² H. Shiba, "Classical spins in superconductors," *Prog. Theor. Phys.* **40**, 435 (1968).
 - ³ Akio Sakurai, "Comments on superconductors with magnetic impurities," *Prog. Theor. Phys.* **44**, 1472 (1970).
 - ⁴ J. Zittartz and E. Müller-Hartmann, "Green's function theory of the Kondo effect in dilute magnetic alloys," *Z. Physik.* **212**, 380 (1968).
 - ⁵ R. Žitko, O. Bodensiek, and Th. Pruschke, "Magnetic anisotropy effects on quantum impurities in superconducting host," *Phys. Rev. B* **83**, 054512 (2011).
 - ⁶ C. P. Moca, E. Demler, B. Jankó, and G. Zaránd, "Spin-resolved spectra of Shiba multiplets from Mn impurities in MgB₂," *Phys. Rev. B* **77**, 174516 (2008).
 - ⁷ A. V. Balatsky, I. Vekhter, and Jian-Xin Zhu, "Impurity-induced states in conventional and unconventional superconductors," *Rev. Mod. Phys.* **78**, 373 (2006).
 - ⁸ J.-D. Pilllet, C. H. L. Quay, P. Morin, C. Bena, A. Levy Yeyati, and P. Joyez, "Andreev bound states in supercurrent-carrying carbon nanotubes revealed," *Nat. Physics* **6**, 965 (2010).
 - ⁹ R S Deacon, Y Tanaka, A Oiwa, R Sakano, K Yoshida, K Shibata, K Hirakawa, and S Tarucha, "Interplay of Kondo and superconducting correlations in the nonequilibrium Andreev transport through a quantum dot," *Physical Review Letters* **104**, 076805 (2010).
 - ¹⁰ Romain Maurand, Tobias Meng, Edgar Bonet, Serge Florens, Laëtitia Marty, and Wolfgang Wernsdorfer, "First-order 0- π quantum phase transition in the Kondo regime of a superconducting carbon-nanotube quantum dot," *Phys. Rev. X* **2**, 011009 (2012).
 - ¹¹ S. H. Ji, T. Zhang, Y. S. Fu, X. Chen, Xu-Cun Ma, J. Li, Wen-Hui Duan, Jin-Feng Jia, and Qi-Kun Xue, "High-resolution scanning tunneling spectroscopy of magnetic impurity induced bound states in the superconducting gap of Pb thin films," *Phys. Rev. Lett.* **100**, 226801 (2008).

- ¹² K. J. Franke, G. Schulze, and J. I. Pascual, “Competition of superconductivity phenomena and Kondo screening at the nanoscale,” *Science* **332**, 940 (2011).
- ¹³ Nino Hatter, Michael Ruby, José I Pascual, Benjamin W Heinrich, and Katharina J Franke, “Magnetic anisotropy in Shiba bound states across a quantum phase transition,” *Nature Communications*, 1–6 (2016).
- ¹⁴ P. Nozières, “Fermi-liquid description of Kondo problem at low temperatures,” *J. Low. Temp. Phys.* **17**, 31 (1974).
- ¹⁵ W. Koller, A. C. Hewson, and D. Meyer, “Singular dynamics of underscreened magnetic impurity models,” *Phys. Rev. B* **72**, 045117 (2005).
- ¹⁶ P. Mehta, N. Andrei, P. Coleman, L. Borda, and G. Zaránd, “Regular and singular Fermi-liquid fixed points in quantum impurity models,” *Phys. Rev. B* **72**, 014430 (2005).
- ¹⁷ A. C. Hewson, *The Kondo Problem to Heavy-Fermions* (Cambridge University Press, Cambridge, 1993).
- ¹⁸ D. C. Mattis, “Symmetry of ground state in a dilute magnetic metal alloy,” *Phys. Rev. Lett.* **19**, 1478 (1968).
- ¹⁹ P. Nozières and A. Blandin, “Kondo effect in real metals,” *J. Phys. (Paris)* **41**, 193 (1980).
- ²⁰ D. M. Cragg, P. Lloyd, and P. Nozières, “On the ground states of some s-d exchange Kondo hamiltonians,” *J. Phys. C: Solid St. Phys.* **13**, 803 (1980).
- ²¹ Y. Oreg and D. Goldhaber-Gordon, “Two-channel Kondo effect in a modified single electron transistor,” *Phys. Rev. Lett.* **90**, 136602 (2003).
- ²² R. M. Potok, I. G. Rau, Hadas Shtrikman, Yuval Oreg, and D. Goldhaber-Gordon, “Observation of the two-channel Kondo effect,” *Nature* **446**, 167 (2007).
- ²³ A. J. Keller, L. Peeters, C. P. Moca, I. Weymann, D. Mahalu, V. Umansky, G. Zaránd, and D. Goldhaber-Gordon, “Universal Fermi liquid crossover and quantum criticality in a mesoscopic system,” *Nature* **526**, 237 (2015).
- ²⁴ Z. Iftikhar, S. Jezouin, A. Anthore, U. Gennser, F. D. Parmentier, A. Cavanna, and F. Pierre, “Two-channel Kondo effect and renormalization flow with macroscopic quantum charge states,” *Nature* **526**, 233 (2015).
- ²⁵ I. Affleck, “Non-Fermi liquid behavior in Kondo models,” *J. Phys. Soc. Japan* **74**, 59 (2005).
- ²⁶ I. Affleck and Andreas W. W. Ludwig, “Critical theory of overscreened Kondo fixed points,” *Nucl. Phys. B* **360**, 641 (1991).
- ²⁷ V. J. Emery and S. Kivelson, “Mapping of the two-channel Kondo problem to a resonant-level model,” *Phys. Rev. B* **46**, 10812 (1992).
- ²⁸ P. Coleman, L. B. Ioffe, and A. M. Tsvelik, “Simple formulation of the two-channel Kondo model,” *Phys. Rev. B* **52**, 6611 (1995).
- ²⁹ Juan M. Maldacena and Andreas W. W. Ludwig, “Majorana fermions, exact mapping between quantum impurity fixed points with four bulk fermion species, and solution of the unitarity puzzle,” *Nucl. Phys. B* **506**, 565 (1997).
- ³⁰ K. G. Wilson, “The renormalization group: Critical phenomena and the Kondo problem,” *Rev. Mod. Phys.* **47**, 773 (1975).
- ³¹ H. R. Krishna-murthy, J. W. Wilkins, and K. G. Wilson, “Renormalization-group approach to the Anderson model of dilute magnetic alloys. I. Static properties for the symmetric case,” *Phys. Rev. B* **21**, 1003 (1980).
- ³² Ralf Bulla, Theo Costi, and Thomas Pruschke, “The numerical renormalization group method for quantum impurity systems,” *Rev. Mod. Phys.* **80**, 395 (2008).
- ³³ Koji Satori, Hiroyuki Shiba, Osamu Sakai, and Yukihiro Shimizu, “Numerical renormalization group study of magnetic impurities in superconductors,” *J. Phys. Soc. Japan* **61**, 3239 (1992).
- ³⁴ D. L. Cox and A. Zawadowski, “Exotic Kondo effects in metals: magnetic ions in a crystalline electric field and tunneling centres,” *Adv. Phys.* **47**, 599 (1998).
- ³⁵ H. B. Pang and D. L. Cox, “Stability of the fixed point of the two-channel Kondo hamiltonian,” *Phys. Rev. B* **44**, 9454 (1991).
- ³⁶ Christian Kolf and Johann Kroha, “Strong versus weak coupling duality and coupling dependence of the Kondo temperature in the two-channel Kondo model,” *Phys. Rev. B* **75**, 045129 (2007).
- ³⁷ The Supplemental Materials contain additional results for the 2CK model, the sub-gap spectra of the three-channel Kondo model and their interpretation in terms of the effective zero-bandwidth model, the conformal field theory discussion of the effect of the pairing operator, and a semi-quantitative calculation of the bound states within the Anderson-Yuval picture.
- ³⁸ T. Hecht, A. Weichselbaum, J. von Delft, and R. Bulla, “Numerical renormalization group calculation of near-gap peaks in spectral functions of the Anderson model with superconducting leads,” *J. Phys. Condens. Mat.* **20**, 275213 (2008).
- ³⁹ Ian Affleck and Andreas W. W. Ludwig, “Universal noninteger ground-state degeneracy in critical quantum systems,” *Phys. Rev. Lett.* **67**, 161 (1991).
- ⁴⁰ G. Yuval and P. W. Anderson, “Exact results for the kondo problem: One-body theory and extension to finite temperature,” *Phys. Rev. B* **1**, 1522–1528 (1970).
- ⁴¹ P. W. Anderson, G. Yuval, and D. R. Hamann, “Exact results in the kondo problem. ii. scaling theory, qualitatively correct solution, and some new results on one-dimensional classical statistical models,” *Phys. Rev. B* **1**, 4464–4473 (1970).
- ⁴² M Fabrizio, AO Gogolin, and P Nozières, “Crossover from non-Fermi-liquid to Fermi-liquid behavior in the two channel Kondo model with channel anisotropy,” *Physical Review Letters* **74**, 4503–4506 (1995).